

Cerebral targeting indicates vagal spread of infection in hamsters fed with scrapie

Michael Beekes,¹ Patricia A. McBride² and Elizabeth Baldauf¹

¹ Robert Koch-Institut, Bundesinstitut für Infektionskrankheiten und nicht übertragbare Krankheiten, FG 123, Nordufer 20, 13353 Berlin, Germany

² Institute for Animal Health, BBSRC/MRC Neuropathogenesis Unit, Ougston Building, West Mains Road, Edinburgh EH9 3JF, UK

The pathogenesis of scrapie and other transmissible spongiform encephalopathies (TSEs) following oral uptake of agent is still poorly understood and can best be studied in mice and hamsters. The experiments described here further extend the understanding of the pathways along which infection spreads from the periphery to the brain after an oral challenge with scrapie. Using TSE-specific amyloid protein (TSE-AP, also called PrP) as a marker for infectivity, immunohistochemical evidence suggested that the first target area in the brain of hamsters

orally infected with scrapie is the dorsal motor nucleus of the vagus nerve (DMNV), rapidly followed by the commissural solitary tract nucleus (SN). The cervical spinal cord was affected only after TSE-AP had been deposited in the DMNV, SN and other medullary target areas. For the first time, these results demonstrate conclusively that, in our animal model, initial infection of the brain after oral ingestion of scrapie agent occurs via the vagus nerve, rather than by spread along the spinal cord.

Introduction

Following the BSE epidemic in Great Britain and the recent emergence of a new CJD variant, transmissible spongiform encephalopathies (TSEs) are a matter of great public concern. The oral route of infection is the epidemiologically most relevant pathway for natural transmission of scrapie and related diseases within and between different species (Diringer *et al.*, 1994). However, little is known about the pathogenesis of TSEs following uptake of infectious agent via the gastrointestinal tract. Previous approaches addressing the dynamics of scrapie pathogenesis by tracing the spread of agent after a parenteral or intragastric challenge in small rodents revealed that infection enters the CNS at the thoracic spinal cord and then spreads rostrally to the brain (Kimberlin & Walker, 1979, 1982, 1986, 1989). However, preliminary observations by Kimberlin & Walker (1982), Muramoto *et al.* (1993) and van Keulen *et al.* (1995) also indicate an alternative spreading pathway, possibly along the vagus nerve. While the existence of an access to the brain bypassing the spinal cord was corroborated recently (Baldauf *et al.*, 1997), the precise

anatomical identity of the bypass remained the subject of speculation. Due to the close association between infectivity and TSE-specific amyloid protein (TSE-AP, also called PrP; McKinley *et al.*, 1983) established in our animal model (Beekes *et al.*, 1996; Baldauf *et al.*, 1997), spread of infection in hamsters can be investigated by tracing the deposition of TSE-AP. In the study described here, we used immunohistochemistry to identify the presence and anatomical location of TSE-AP as an indicator for the spread of infection to and within the brain of hamsters orally challenged with scrapie. This approach allowed an exact localization of the initial cerebral target areas and provided strong evidence for the vagus nerve as the primary pathway to the brain in our model animals.

Methods

■ Oral infection of outbred Syrian Golden hamsters with scrapie (strain 263K) was performed as described previously (Baldauf *et al.*, 1997). Four animals were sacrificed at 84, 91, 98, 105, 113, 119, 126 and 133 days post-infection (p.i.), and also at 156 days p.i. (terminal stage of disease). Four uninfected controls were sacrificed after having reached an age of between 180 and 210 days. Brain and vertebral column were removed. Two of the brains from each group were dissected mid-sagittally, the two others were dissected coronally into five segments. The spinal column

Author for correspondence: Michael Beekes.
Fax +49 30 4547 2609. e-mail BeekesM@rki.de

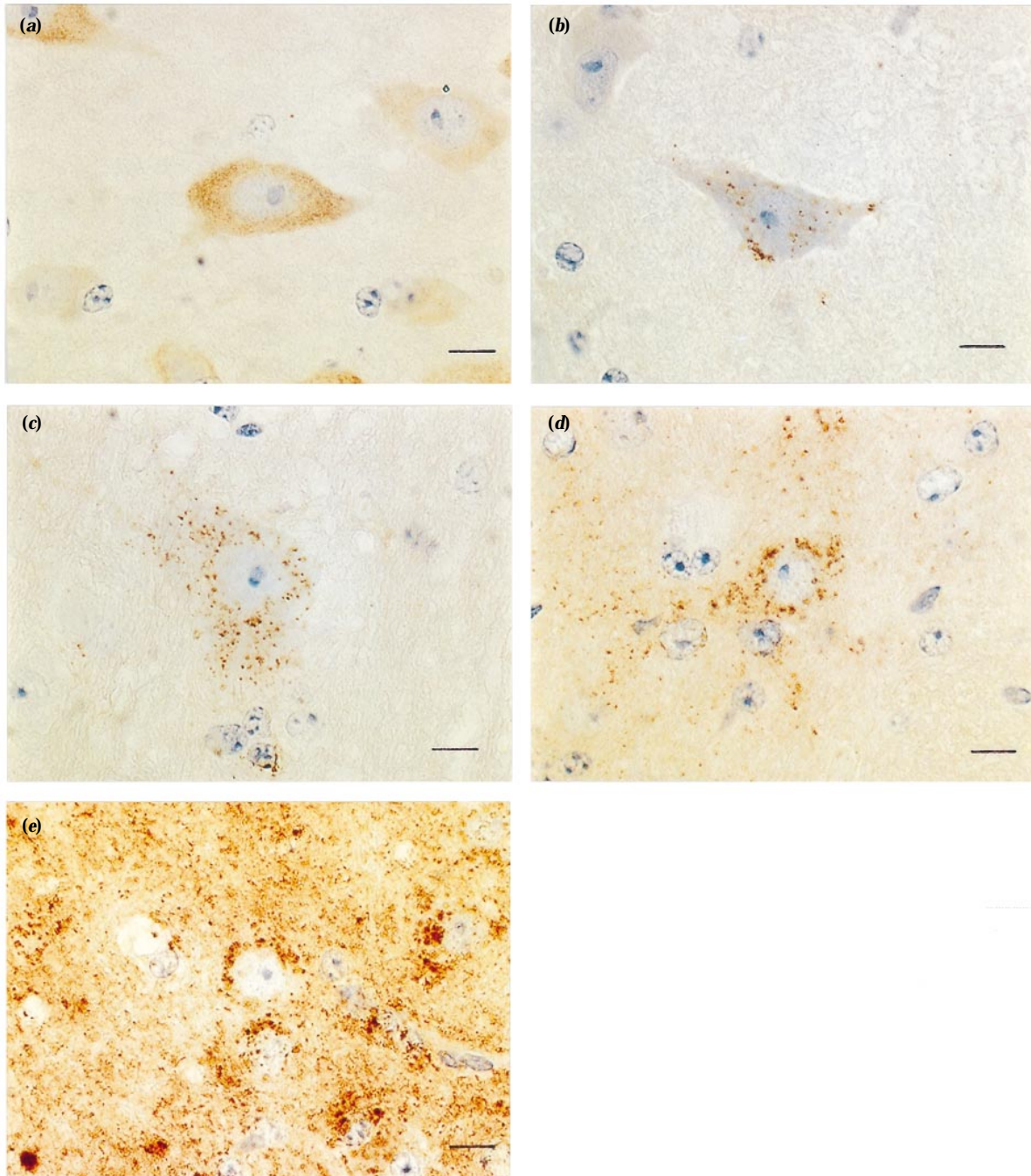


Fig. 1. Immunohistochemical appearance of TSE-AP in the CNS. (a) Unaffected control. Cellular precursor protein (homogeneous brown staining) within neurons. Some neurons remain unstained. (b) Early stage of infection. Punctate deposits of abnormal protein appear within and on cell surface of individual cells. (c) Inclusions progressively increase in number and staining intensity. (d) As incubation period advances, heavier deposits accumulate around cells and appear scattered in the neuropil. (e) Terminal stage of disease. TSE-AP deposition is consolidated within the neuropil. Bar, 10 μ m.

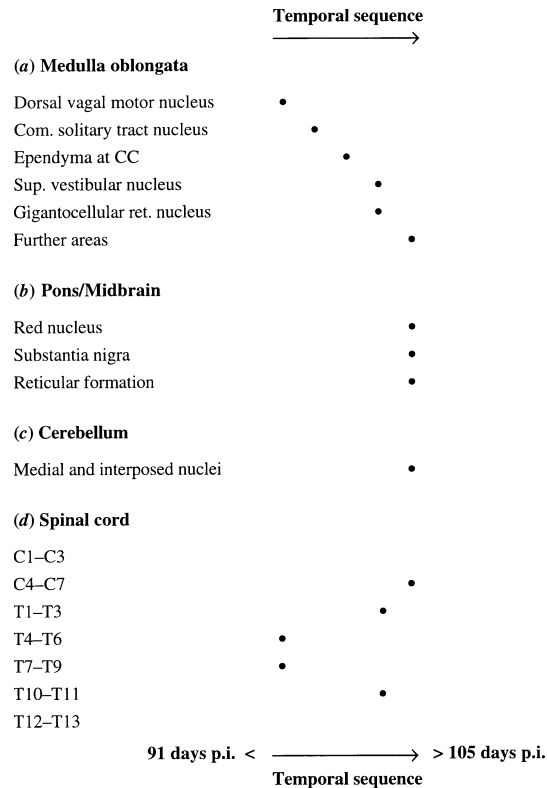


Fig. 2. Early target areas in the CNS found to be affected between 91 and 105 days p.i. Dots indicate the temporal sequence of TSE-AP deposition. Spinal cord segments C1–C3 and T12–T13 showed no immunostaining for the pathological protein until 105 days p.i. (a) 'Further areas' in the medulla oblongata: IO and DAO, PRN, LPGN, SpVN and MVN. (b) 'Reticular formation': RaN and PoN.

was dissected transversally into segments corresponding to vertebrae C1–C3, C4–C7, T1–T3, T4–T6, T7–T9, T10–T11 and T12–T13 and the spinal cord was removed. Tissue samples were fixed in paraformaldehyde–lysine–periodate (2% paraformaldehyde in final concentration), dehydrated over 6 h and embedded in paraffin wax. Serial and/or semi-serial sections were cut at 6 μ m. Immunostaining was carried out according to the peroxidase antiperoxidase (PAP) and/or ABC method using MAb 3F4 (Kasczak *et al.*, 1987) to label TSE-AP and its normal precursor and diaminobenzidine (DAB) to visualize the reaction product. Prior to immunostaining, sections were pretreated with formic acid (98%) for 10 min to enhance staining. Adjacent sections were stained with cresyl violet (0.1%) and haematoxylin and eosin to facilitate neuro-anatomical identification.

Results

TSE-AP presented as granular accumulations of immunoreactive material within or around neurons. These infection-specific deposits could be clearly distinguished from the normal precursor protein and were absent in uninfected control animals (Fig. 1).

As in previous studies (Beekes *et al.*, 1996; Baldauf *et al.*,

1997), formation of TSE-AP in the CNS was first seen at 91 days p.i., but onset varied between individuals. However, the sequence of areas targeted in the brain and spinal cord was remarkably consistent (Figs 2 and 3 *a–f*, *g–l*).

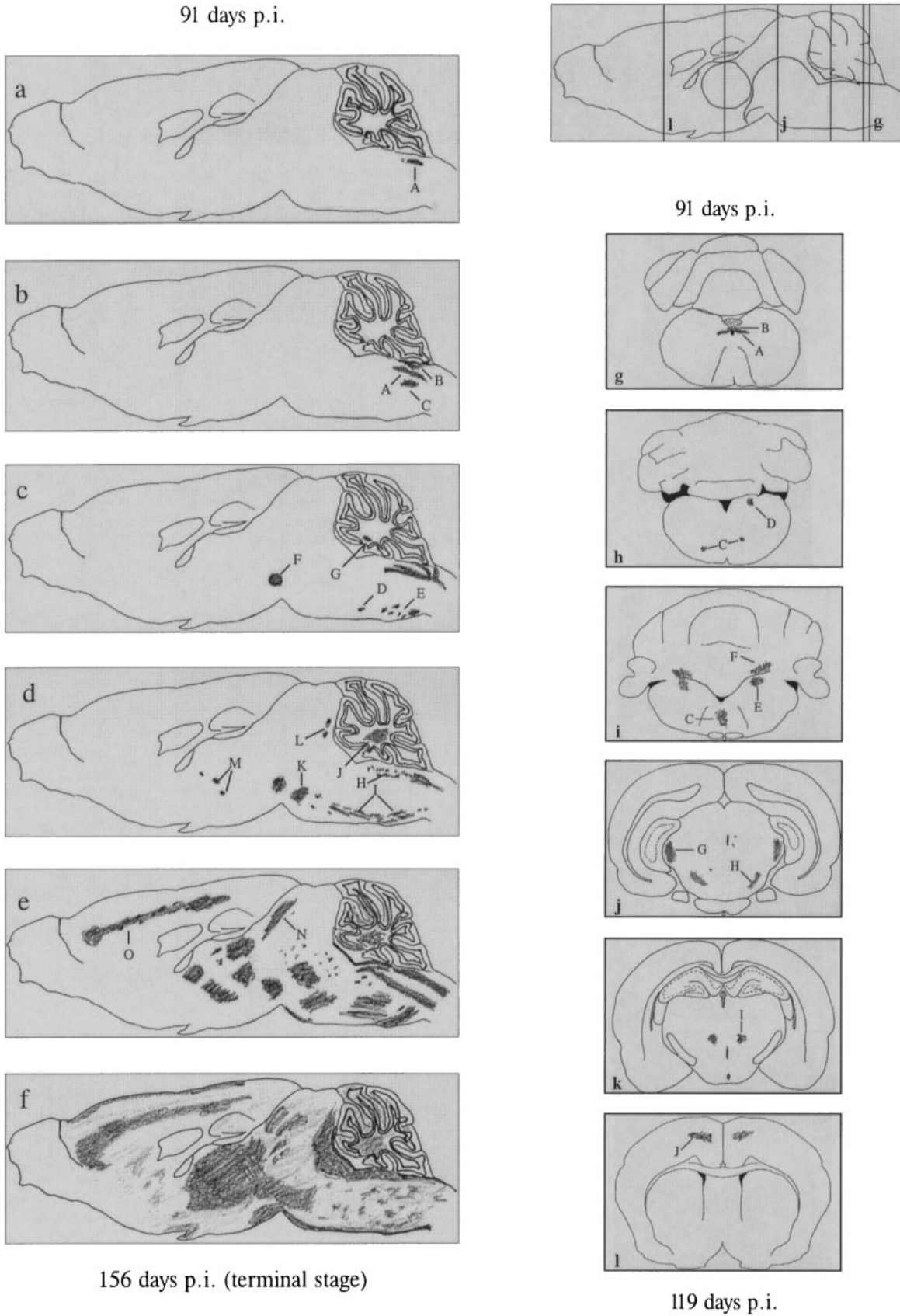
The first area showing deposition of TSE-AP in the brain was the dorsal motor nucleus of the vagus nerve (DMNV; Fig. 4*a*), followed by the commissural solitary tract nucleus (SN) and ependymal linings of the adjacent central canal (CC; Fig. 4*b*). Positive immunostaining extended caudally to the area postrema (AP) although the AP was itself negative. Shortly after detection in the DMNV and SN (Fig. 4*c*), TSE-AP appeared in the superior vestibular nucleus (SVN) and in the gigantocellular nucleus (GN) of the reticular formation.

Subsequently, TSE-AP was seen in other nuclei of the medulla [spinal and medial vestibular nuclei (SpVN, MVN), parvocellular reticular nucleus (PRN), inferior and dorsal accessory olives (IO, DAO), lateral paragigantocellular nucleus (LPGN); Fig. 4*d*], in the pons and midbrain [red nucleus (RN), substantia nigra, raphe and pontine nuclei of the reticular formation (RaN, PoN)] and in the cerebellum [medial and interposed nuclei (MCN, ICN); Fig. 4*e*]. The rapid spread of infection did not allow the identification of a clear temporal sequence in these later target areas. The trend of further spread was in a caudal to rostral direction. At 113 days p.i., TSE-AP could be detected for the first time in the ventromedial thalamic nucleus (VnTN) and by 119 days p.i. it was seen in the medial geniculate nucleus (MGN) and throughout the thalamus (Fig. 4*f*) and hypothalamus. At this time TSE-AP also appeared in the parietal, cingulate (CCo) and frontal cortex (FCo). At 133 days p.i. deposition of TSE-AP had spread considerably within individual areas. By 156 days p.i., when the disease reached its clinical stage, the pathological protein was widespread throughout all brain areas except the olfactory lobes.

In the spinal cord, the first deposition of TSE-AP appeared in and around the neuronal cell bodies of the grey matter between vertebrae T4–T9. Timing of appearance coincided with that in the brain: the first deposition was seen at 91 days p.i. in the same cases and with corresponding relative amounts as had been identified in the brain. Subsequent spread within the spinal cord (Fig. 2) occurred in a rostral and caudal direction as reported previously (Kimberlin & Walker, 1979, 1982, 1986, 1989; Beekes *et al.*, 1996; Baldauf *et al.*, 1997). However, TSE-AP was found in the cervical spinal cord (C1–C3) only after it had been identified in a number of target areas in the medulla.

Discussion

These findings suggest that the onset of infection in the medulla oblongata is not accounted for by rostral spread along the grey matter of the spinal cord. Early infection of the DMNV and SN via white matter tracts also appears to be unlikely as no tracts directly link the thoracic spinal cord with



these medullary nuclei. Thus, the initial appearance of TSE-AP in the DMNV and SN strongly indicates that infection enters the brain via anatomical projections outside the CNS. Spread via parasympathetic efferent or associated afferent fibres of the vagus nerve (cranial nerve X) best fits the observed sequence of initial target areas in the medulla oblongata. Vagal efferents and afferents have their respective nerve cell bodies in the DMNV and in the nodosal ganglion (NG). However, the afferent fibres do not terminate in the NG but run to the solitary tract nucleus where they synapse with perikarya of interneurons directly projecting to vagal motor neurons in the DMNV (see Card *et al.*, 1993; Standish *et al.*, 1994). Efferents and afferents of this vagal circuit innervate the heart and the lung and visceral organs of the digestive system such as the stomach, pancreas, small intestine and ascending colon.

Therefore, neuroanatomically, the sequence of target areas can best be explained by a retrograde spread of infection along parasympathetic vagal efferents to the DMNV and subsequently to the solitary tract nucleus as described for pseudorabies virus (Card *et al.*, 1993; Standish *et al.*, 1994). However, direct spread to the SN along visceral vagal afferents from the gastro-intestinal tract or along afferents of the vagus and other cranial nerves from the pharynx (IX, X), larynx (X) and tongue (VII, IX, X) is also possible, but not suggested by the observed timing of events.

Other areas showing early deposition of TSE-AP in the brain, i.e. the SVN, GN and ependymal linings of the CC and fourth ventricle, may well be infected via neuronal pathways originating or terminating in the DMNV and SN. The onset of infection observed in target areas located within the vestibular nuclei could be explained by spread from the DMNV and SN along fibres of the vestibulo-autonomic reflex (Balaban & Beryozkin, 1994; Ito & Honjo, 1990). Projections from the GN to pancreatic parasympathetic neurons originating in the

DMNV (Loewy *et al.*, 1994) could account for spread to the GN. Early deposition of TSE-AP in the ependyma of the CC at the fourth ventricle could possibly also be explained by projections to or from the DMNV (Navaratnam & Lewis; 1975) and SN. However, these areas lie anatomically adjacent to one another (Fig. 3g) and direct cell-to-cell spread also appears possible. In any case, subsequent spread of infection from the early target sites in the medulla to prominent nuclei in the pons, midbrain, cerebellum and thalamus seems to follow well-established neuroanatomical pathways (Andrezik & Beitz, 1985; Flumerfelt & Hryciyshyn, 1985).

The findings reported here expand our understanding of scrapie invasion of the CNS which, until recently (Baldauf *et al.*, 1997), focused predominantly on the spinal cord (Kimberlin & Walker, 1979, 1982, 1986, 1989). Our results indicate an important role of the autonomic nervous system in the spread of infection and striking similarities between the routing pathways of scrapie agent and pseudorabies virus (Card *et al.*, 1993; Standish *et al.*, 1994). Further studies will be necessary to investigate more thoroughly the relationship between TSEs and neurodegenerative diseases caused by conventional viruses.

Most recently, Blättler *et al.* (1997) reported that neuroinvasion of the scrapie agent is dependent on 'PrP expression' in a tissue compartment interposed between the lymphoreticular system and the CNS. The findings outlined above strongly point to the vagus nerve as an integral part of this compartment.

We would like to extend our special thanks to Prof. Dr H. Diring for critical reading of the manuscript and for helpful discussion. The skilful technical assistance of Ms M. Wilson is gratefully acknowledged. This work was supported by grants to H. Diring from the European Union, the Bundesministerium für Bildung, Wissenschaft, Forschung und Technologie, and the Hertie-Stiftung.

Fig. 3. (a–f) Sequence of cerebral target areas observed in semi-serial mid-sagittal sections. Deposition of TSE-AP (shaded regions) is represented in brain maps of selected individual slices covering the range between first appearance (91 days p.i.) and terminal accumulation (156 days p.i.). A, DMNV; B, SN; C, PRN; D, GN; E, IO; F, RN; G, MCN; H, SpVN, MVN and SVN; I, medullary and pontine reticular nuclei (IO, GN, PoN); J, MCN and ICN; K, retrorubral field; L, central grey matter; M, ventrolateral thalamic nucleus and VmTN; N, superior colliculus; and O, CCo (layers 4 and 5). (g–l) Initial target areas at different coronal levels. Deposition of TSE-AP (shaded regions) is represented in brain maps of selected individual slices demonstrating the caudal to rostral spread observed between 91 and 119 days p.i. A, DMNV; B, SN; C, GN; D, SpVN; E, SVN; F, MCN and ICN; G, MGN; H, retrorubral field; I, VmTN; and J, CCo and FCo (layers 4 and 5).

Fig. 4. Immunolabelling of TSE-AP (brown staining) in various target areas of the brain. Photographs were taken from selected slices of brains from individual animals sacrificed at different times p.i. (a) and (b), Earliest target sites. DMNV (a) and SN (larger arrowheads) and CC (smaller arrowhead) (b) at 91 days p.i. Bar, 20 µm. (c) Accumulation in the DMNV (larger arrowheads) and in the SN (smaller arrowheads) later in incubation period, 126 days p.i. Bar, 200 µm. (d) Deposition in several medullary nuclei, 119 days p.i. Bar, 400 µm. (e) Cerebellar target sites in the MCN and ICN (larger arrowheads) and portions of the granular layer (smaller arrowheads), 119 days p.i. Bar, 200 µm. (f) Widespread brainstem deposition at terminal stage of disease particularly in the thalamus (larger arrowheads) and RN (smaller arrowheads), 156 days p.i. Bar, 400 µm.

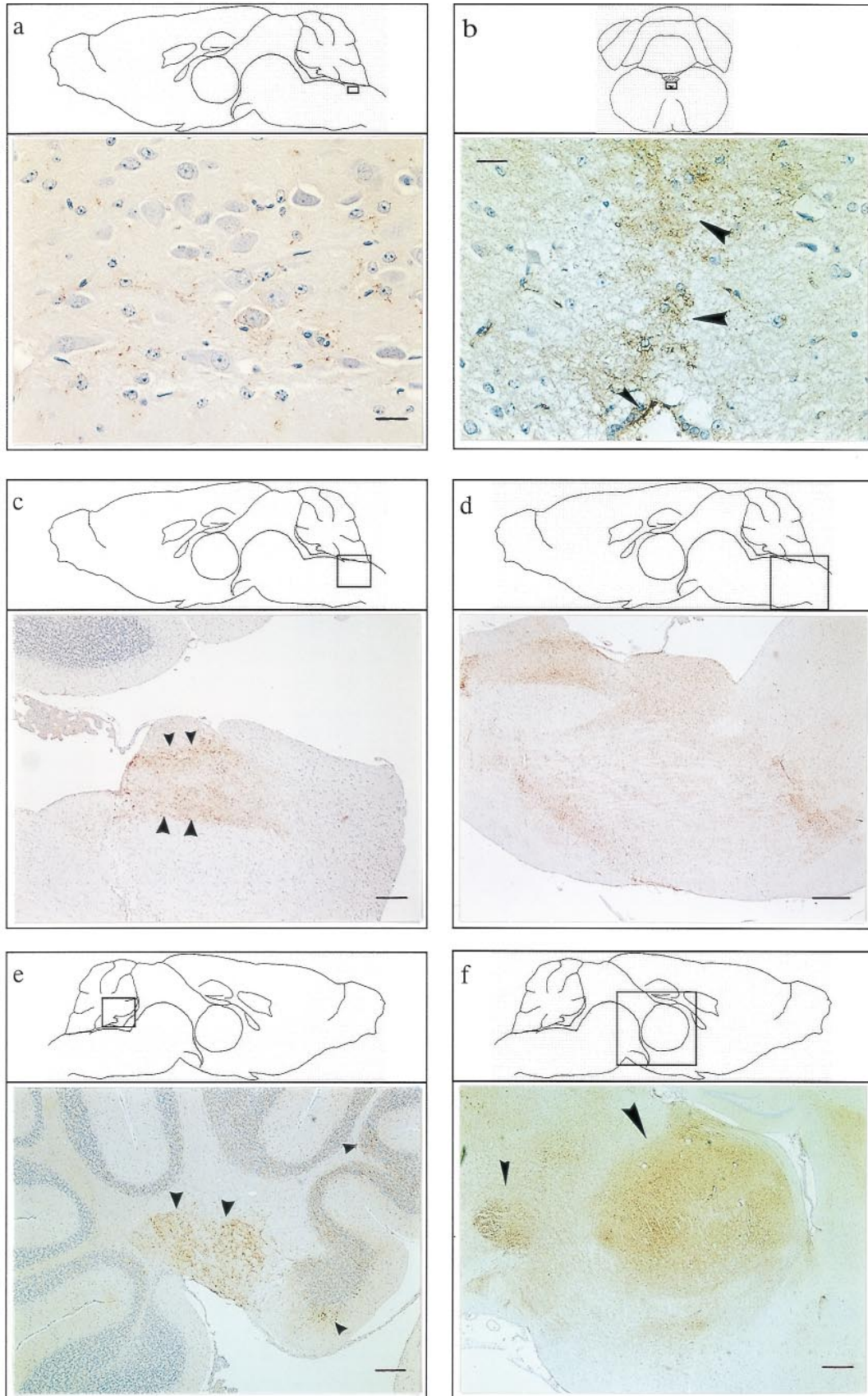


Fig. 4. For legend see page 605.

References

- Andrejik, J. A. & Beitz, A. J. (1985).** Reticular formation, central gray and related tegmental nuclei. In *The Rat Nervous System*, vol. 2, pp. 1–28. Edited by G. Paxinos. Sidney: Academic Press.
- Balaban, C. D. & Beryozkin, G. (1994).** Vestibular nucleus projections to nucleus tractus solitarius and the dorsal motor nucleus of the vagus nerve: potential substrates for vestibulo-autonomic interactions. *Experimental Brain Research* **98**, 200–212.
- Baldauf, E., Beekes, M. & Diring, H. (1997).** Evidence for an alternative direct route of access for the scrapie agent to the brain bypassing the spinal cord. *Journal of General Virology* **78**, 1187–1197.
- Beekes, M., Baldauf, E. & Diring, H. (1996).** Sequential appearance and accumulation of pathognomonic markers in the central nervous system of hamsters orally infected with scrapie. *Journal of General Virology* **77**, 1925–1934.
- Blättler, T., Brandner, S., Raeber, A. J., Klein, M. A., Voigtländer, T., Weissmann, Ch. & Aguzzi, A. (1997).** PrP-expressing tissue required for transfer of scrapie infectivity from spleen to brain. *Nature* **389**, 69–72.
- Card, J. P., Rinaman, L., Lynn, R. B., Lee, B.-H., Meade, R. P., Miselis, R. R. & Enquist, L. W. (1993).** Pseudorabies virus infection of the rat central nervous system: ultrastructural characterization of viral replication, transport, and pathogenesis. *The Journal of Neuroscience* **13**, 2515–2539.
- Diring, H., Beekes, M. & Oberdieck, U. (1994).** The nature of the scrapie agent: the virus theory. *Annals of the New York Academy of Sciences* **724**, 246–258.
- Flumerfelt, B. A. & Hrycyshyn, A. W. (1985).** Precerebellar nuclei and red nucleus. In *The Rat Nervous System*, vol. 2, pp. 221–250. Edited by G. Paxinos. Sidney: Academic Press.
- Ito, J. & Honjo, I. (1990).** Central fiber connections of the vestibulo-autonomic reflex arc in cats. *Acta Oto-Laryngologica* **110**, 379–385.
- Kasczak, R. J., Rubenstein, R., Merz, P. A., Tonna-Demasi, M., Fersko, R., Carp, R. I., Wisniewski, H. M. & Diring, H. (1987).** Mouse polyclonal and monoclonal antibody to scrapie-associated fibril protein. *Journal of Virology* **61**, 3688–3693.
- Kimberlin, R. H. & Walker, C. A. (1979).** Pathogenesis of mouse scrapie: dynamics of agent replication in spleen, spinal cord and brain after infection by different routes. *Journal of Comparative Pathology* **89**, 551–562.
- Kimberlin, R. H. & Walker, C. A. (1982).** Pathogenesis of mouse scrapie: patterns of agent replication in different parts of the CNS following intraperitoneal infection. *Journal of the Royal Society of Medicine* **75**, 618–624.
- Kimberlin, R. H. & Walker, C. A. (1986).** Pathogenesis of scrapie (strain 263K) in hamsters infected intracerebrally, intraperitoneally or intracocularly. *Journal of General Virology* **67**, 255–263.
- Kimberlin, R. H. & Walker, C. A. (1989).** Pathogenesis of scrapie in mice after intragastric infection. *Virus Research* **12**, 213–220.
- Loewy, A. D., Franklin, M. F. & Haxhiu, M. A. (1994).** CNS monoamine cell groups projecting to pancreatic vagal motor neurons: a transneuronal labeling study using pseudorabies virus. *Brain Research* **638**, 248–260.
- McKinley, M. P., Bolton, D. C. & Prusiner, S. B. (1983).** A protease-resistant protein is a structural component of the scrapie prion. *Cell* **35**, 57–62.
- Muramoto, T., Kitamoto, T., Tateishi, J. & Goto, I. (1993).** Accumulation of abnormal prion protein in mice infected with Creutzfeldt–Jakob disease via intraperitoneal route: a sequential study. *American Journal of Pathology* **143**, 1470–1479.
- Navaratnam, V. & Lewis, P. R. (1975).** Effects of vagotomy on the distribution of cholinesterases in the cat medulla oblongata. *Brain Research* **100**, 599–613.
- Standish, A., Enquist, L. W. & Schwaber, J. S. (1994).** Innervation of the heart and its central medullary origin defined by viral tracing. *Science* **263**, 232–234.
- van Keulen, L. J. M., Schreuder, B. E. C., Muelen, R. H., Poelen-vanden Berg, M., Mooij-Harkes, G., Vromans, M. E. W. & Langeveld, J. P. M. (1995).** Immunohistochemical detection and localization of prion protein in brain tissue of sheep with natural scrapie. *Veterinary Pathology* **32**, 299–308.

Received 12 September 1997; Accepted 16 October 1997